JVI
Journals.ASM.org

Defining the Chemokine Basis for Leukocyte Recruitment during Viral Encephalitis

Daniela Michlmayr,[a] Clive S. McKimmie,[a] Marieke Pingen,[a] Ben Haxton,[b] Karen Mansfield,[b] Nicholas Johnson,[b] Anthony R. Fooks,[b] Gerard J. Graham[a]

Centre for Immunobiology, Institute of Infection, Immunity and Inflammation, College of Medical, Veterinary and Life Sciences, University of Glasgow, Glasgow, United Kingdom[a]; Animal Health and Veterinary Laboratories Agency, Addlestone, United Kingdom[b]

ABSTRACT

The encephalitic response to viral infection requires local chemokine production and the ensuing recruitment of immune and inflammatory leukocytes. Accordingly, chemokine receptors present themselves as plausible therapeutic targets for drugs aimed at limiting encephalitic responses. However, it remains unclear which chemokines are central to this process and whether leukocyte recruitment is important for limiting viral proliferation and survival in the brain or whether it is predominantly a driver of coincident inflammatory pathogenesis. Here we examine chemokine expression and leukocyte recruitment in the context of avirulent and virulent Semliki Forest virus (SFV) as well as West Nile virus infection and demonstrate rapid and robust expression of a variety of inflammatory CC and CXC chemokines in all models. On this basis, we define a chemokine axis involved in leukocyte recruitment to the encephalitic brain during SFV infection. CXCR3 is the most active; CCR2 is also active but less so, and CCR5 plays only a modest role in leukocyte recruitment. Importantly, inhibition of each of these receptors individually and the resulting suppression of leukocyte recruitment to the infected brain have no effect on viral titer or survival following infection with a virulent SFV strain. In contrast, simultaneous blockade of CXCR3 and CCR2 results in significantly reduced mortality in response to virulent SFV infection. In summary, therefore, our data provide an unprecedented level of insight into chemokine orchestration of leukocyte recruitment in viral encephalitis. Our data also highlight CXCR3 and CCR2 as possible therapeutic targets for limiting inflammatory damage in response to viral infection of the brain.

IMPORTANCE

Brain inflammation (encephalitis) in response to viral infection can lead to severe illness and even death. This therefore represents an important clinical problem and one that requires the development of new therapeutic approaches. Central to the pathogenesis of encephalitis is the recruitment of inflammatory leukocytes to the infected brain, a process driven by members of the chemokine family. Here we provide an in-depth analysis of the chemokines involved in leukocyte recruitment to the virally infected brain and demonstrate that simultaneous blockade of two of these receptors, namely, CXCR3 and CCR2, does not alter viral titers within the brain but markedly reduces inflammatory leukocyte recruitment and enhances survival in a murine model of lethal viral encephalitis. Our results therefore highlight chemokine receptors as plausible therapeutic targets in treating viral encephalitis.

The brain possesses highly developed neuronal circuits, the majority of which cannot be easily replaced if lost or damaged as a result of, for example, virally induced encephalitis. As a consequence, central nervous system (CNS) immune responses are tightly controlled (1); antibodies, complement, proinflammatory cytokines, leukocytes, and major histocompatibility complex class I (MHC-I) expression are generally absent, although rare circulating T cells can be found in the cerebrospinal fluid (CSF) (2). The apparent immunosuppressive nature of the CNS is maintained by a sophisticated series of mechanisms that prevents the unwanted access of plasma components and bone marrow-derived leukocytes. Nonetheless, despite the absence of typical immune sentinels and a lymphatic network, florid and life-threatening CNS immune responses can occur during infection with encephalitic pathogens, especially viruses. Although mouse models of viral encephalitides have been well described, such as those using infection with Semliki Forest virus (SFV), lymphocytic choriomeningitis virus (LCMV), and West Nile virus (WNV), the mechanisms by which leukocytes enter the infected brain are not well understood. Additionally, their contribution to clearing CNS virus, modulating neuropathogenesis, or host survival has not yet been properly defined (3–6). Developing our understanding of this key aspect of the encephalitic process is central to our ability to therapeutically manipulate it.

Chemokines are key chemotactic cytokines that control and drive leukocyte migration (7–9) and interact with target cells through receptors belonging to the 7-transmembrane-spanning family of G-protein-coupled receptors (10, 11). Without chemokines, coordinated immune responses cannot occur. Microbial infection of the CNS can trigger substantial chemokine expression by both glia and neurons (12, 13), although the function and hierarchical relevance of these chemokines in attracting relevant an-

Received 20 November 2013 **Accepted** 22 May 2014
Published ahead of print 4 June 2014
Editor: M. S. Diamond
Address correspondence to Clive McKimmie, Clive.McKimmie@glasgow.ac.uk, or Gerard J. Graham, Gerard.Graham@glasgow.ac.uk.

doi:10.1128/JVI.03421-13

tiviral leukocyte subsets have yet to be fully elucidated (14, 15). Chemokine-mediated influx of leukocytes into the brain can act to clear infections but can also be responsible for deleterious bystander neuronal damage associated with morbidity and, in some cases, increased mortality. The final outcome of encephalitis, whether progressive incapacitation of the host or resolution, will depend on the infecting pathogen, such as viruses, and a range of host factors, including age and immune status. In murine models, this is perhaps best exemplified by CXCR3-deficient mice, which display enhanced CNS viral titers, and mortality, following infection with WNV. In stark contrast, these mice are protected from the otherwise lethal infection with LCMV or cerebral malaria (16, 17). Likewise, a putative role for CCR5 in host defense has been suggested in the context of effective immune responses to WNV, although CCR5 is dispensable for responses to LCMV (18–20). Thus, host chemokine responses can be beneficial in terms of pathogen removal, but often at the cost of facilitating bystander damage. In each scenario, the outcome of the infection will most likely depend on the relative contributions to pathogenesis by direct pathogen-mediated damage and indirect immunopathology. Importantly, drawing firm conclusions on the chemotactic basis by which leukocytes enter CNS tissue is difficult when using gene-deficient mice, in which deficiency in a particular chemokine receptor (CKR) may exert its influence at multiple stages of an immune response, including the process by which leukocytes enter the CNS. Additionally, gene deficiency cannot be modulated or varied during the disease, and consequently small-molecule blockers against specific chemokine receptors were used instead to identify their role in the pathogenesis of viral encephalitis.

Therefore, in an attempt to more fully understand the regulation of leukocyte recruitment into virus-infected brain and to complement previous studies in this area (21–23), we have used mouse models of viral encephalitis to define, in unprecedented detail, the form and magnitude of the chemotactic cues expressed by the virus-infected brain and the kinetics of entry of distinct leukocyte populations in relation to chemokine expression. Importantly, for the first time, we have utilized a panel of CKR antagonists to evaluate the hierarchy and relative importance of distinct chemokines for CNS leukocyte influx. Together, this comprehensive analysis identifies the CXCR3 axis as being the key instigator of CNS inflammation in response to alphavirus infection, placing it at the top of a hierarchical cascade that is followed by CCR2- and CCR5-mediated processes. Furthermore, we show that therapeutic blockade of two chemokine receptors, CCR2 and CXCR3, provides a significant survival advantage in models of virulent, lethal viral infection. Chemokine receptors therefore represent plausible therapeutic targets in viral encephalitis.

MATERIALS AND METHODS

Mice and virus infection. Female C57BL/6 mice were purchased from Harlan (Blackthorne, United Kingdom), maintained at the University of Glasgow Central Research Facility (CRF) under pathogen-free conditions, and used between 8 and 12 weeks of age. Female CD1 mice were purchased from Charles River (Margate, United Kingdom) and maintained at the Animal Health and Veterinary Laboratories Agency (AHVLA, Weybridge, United Kingdom). All procedures were carried out in accordance with the United Kingdom Home Office regulations under the compliance of the appropriate project and personal licenses.

Viral infection. For studies using SFV as a model of infection, C57BL/6 mice were injected intraperitoneally (i.p.) with 5×10^3 PFU of SFV strain A7(74) or 2×10^5 PFU of SFV strain L10 suspended in phosphate-buffered saline with 0.75% bovine serum albumin (PBSA) or PBSA only (mock infected). The virus was kindly provided by John Fazakerley (The Pirbright Institute, Pirbright, United Kingdom). Mice were sampled on postinfection days (PID) 3, 4, 5, 7, and 10. For studies using WNV as a model of infection, CD1 mice were inoculated under isoflurane anesthesia with 1×10^4 PFU of WNV strain NY99 suspended in 20 μl of Eagle's minimal essential medium (EMEM) via the intranasal route (i.n.). Control mice were inoculated with EMEM only. Mice were sampled on PID 2, 4, and 6. All WNV experiments were carried out in an animal biosafety level 3 facility at the Animal Health and Veterinary Laboratories Agency (Weybridge, United Kingdom).

RNA extraction and qRT-PCR. Total RNA was extracted from homogenized brain tissue using TRIzol Plus RNA with on-column DNA digestion (Life Tech). One to 2 μg of total RNA was converted to cDNA using the QuantiTect reverse transcription (RT) kit (Qiagen) using random primers and oligo(dT) primers. Viral RNA was extracted from plasma of SFV-infected mice using the QIAamp viral RNA minikit (Qiagen) and converted into cDNA using the high-capacity RNA-to-cDNA kit (Applied Biosystems). Analysis of the relationship between the amount of viral nsp3 transcript measured and the numbers of PFU revealed that approximately 10 nsp3 transcripts equated to 1 PFU (Fig. 1H). Real-time PCR was performed as described previously (24, 25), and samples were tested in triplicate using cDNA (1 μg total RNA transcribed), 2× PerfeCTa SYBR green fast mix (Quanta Bioscience), 500 μM forward and reverse primer mix, and RNase-free water according to the manufacturer's protocol. All primers used for quantitative RT-PCR (qRT-PCR) were designed using Primer 3 software and manufactured by IDT technologies. A list of all primers is available upon request. The samples were run on a 7900HT real-time PCR machine (Applied Biosystems) for 40 cycles. The absolute copy number was calculated by using standards as previously described and normalized to the number of copies of the reference gene encoding TATA binding protein (TBP) (26).

TaqMan low-density array analysis. Custom TaqMan array microfluidic cards (Applied Biosystems) containing probes and primers for 32 (for SFV tissue analysis) or 64 (for WNV tissue analysis) genes were loaded with a 100-μl reaction mixture consisting of cDNA (300 to 562 ng total RNA equivalent), RNase-free water, and 2× TaqMan Universal PCR master mix (Applied Biosystems). The TaqMan array cards were briefly spun down at 200 × *g* for 1 min and then run on a 7900HT fast real-time machine for 40 cycles. Data were analyzed using SDS 2.2 software and RQ Manager according to the manufacturer's instructions (Applied Biosystems). The relative copy number of each target gene was double normalized to an endogenous reference gene [*18S* for A7(74) samples and *Eif3f* for L10 samples] and to a calibrator sample (uninfected mouse brain) using the $\Delta\Delta C_T$ method (where C_T is threshold cycle) (27).

Isolation of mononuclear cells from the CNS. Mononuclear cells were isolated from half mouse brains as previously described (28). In brief, brains (pooled from 5 to 10 mice) were finely minced and digested in Hanks' buffered salt solution (HBSS; Gibco, United Kingdom) containing DNase I (5 U/ml; Sigma-Aldrich) and Liberase TM medium research grade (0.03 Wünsch U/ml; Roche) for 60 min at 37°C. Digestion was quenched in rinsing buffer containing HBSS, 0.5% fetal calf serum (FCS), and 2 mM EDTA (Sigma). The subsequent homogenate was then passed through a 70-μm cell strainer (BD Biosciences). The brain cells were washed twice with rinsing buffer and resuspended in Percoll and HBSS to obtain a 30% Percoll solution. The 30% solution was then layered over 70% Percoll and spun down at 2,000 × *g* for 20 min at room temperature. Mononuclear cells were collected from the interphase, washed in fluorescence-activated cell sorter (FACS) buffer containing PBS, 0.5% FCS, and 2 mM EDTA, and counted with a hemocytometer using trypan blue staining for cell viability.

Flow cytometry. Isolated mononuclear cells were incubated with anti-mouse CD16/CD32 Fc-block (Miltenyi) diluted 1:20 in FACS buffer for 10 min before staining with primary antibodies conjugated with fluorophores and appropriate isotypes (a list of the antibodies is available upon

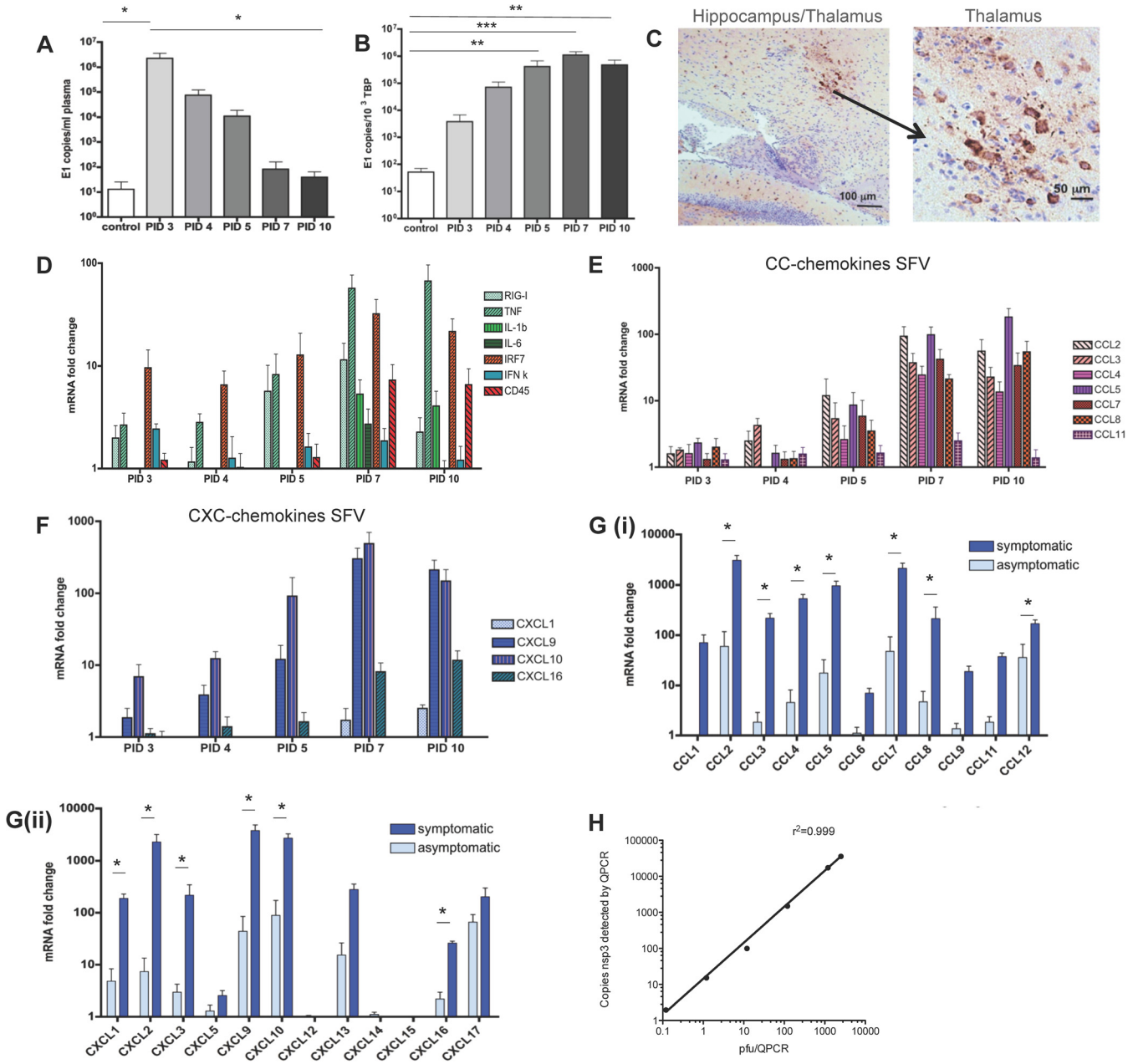

FIG 1 The cytokine and chemokine response to avirulent and virulent SFV infection. (A and B) QPCR analysis of SFV A7 (74) viral titers in peripheral blood and brain of infected mice at the indicated time points following viral inoculation. Data are presented as numbers of copies of E1 transcript per ml of plasma or per 10^3 copies of the housekeeping TBP gene. (C) Immunostaining for SFV in brain sections of SFV-infected mice indicating staining (brown) in the hippocampus/thalamus at low (left panel) or high (right panel) magnification. (D to F) TaqMan low-density array analysis of inflammatory cytokine, interferon response gene, and CD45 expression (D), CC chemokines (E), and CXC chemokines (F) in brains of SFV A7 (74)-infected mice at the indicated time points following viral inoculation. (G) TaqMan low-density array analysis of inflammatory CC (i) and CXC chemokine (ii) expression in the brains of mice either displaying or not displaying symptoms postinfection with the virulent L10 strain of SFV. Data are expressed as relative fold changes in healthy control mouse brains. (H) Correlation between copy number of SFV nsp3 transcripts as detected by QPCR and PFU as measured by routine plaque-forming assays. Each sample was tested in triplicate with 4 to 7 mice per time point. Significance was determined by Student's *t* test (*, $P < 0.05$) (G) and by the Kruskal-Wallis test with Dunn's posttest (**, $P < 0.01$; ***, $P < 0.001$) (A and B).

request). Cells isolated from mice infected with SFV strain L10 were fixed using BD Cytofix/Cytoperm solution and incubated for 10 min on ice. DRAQ7-APC-Cy7 (Biostatus) or Fixable Viability dye-APC-Cy7 (eBioscience) for fixed cells was used for live/dead cell exclusion. FACS data were collected on the MACSQuant machine (Miltenyi), and analysis was performed using FlowJo version 8.8.7 (Tree Star Inc., USA). A total of 1×10^6 to 5×10^6 events were captured for each analysis. All samples were gated on the live CD45 high (leukocyte) cell population, and cell doublets were excluded using forward scatter (height) (FSC-H) and FSC (area) (FSC-A).

Immunohistochemistry. Half mouse brains were removed from the skull and immediately fixed in a 4% paraformaldehyde (PFA) solution (Santa Cruz) for 24 h at 4°C. The brains were then transferred to 70% ethanol, processed using an automated tissue processor (Shandon Citadel

1000; Thermo Scientific), and embedded in paraffin. Sections were then cut at 5 to 6 μm using a Shandon Finesse 325 microtome (Thermo Scientific). After rehydration of brain sections, antigen retrieval was performed by boiling sections in the microwave for 8 min in 10 mM citrate buffer at pH 6. The sections were then blocked with 20% horse serum (Vector laboratories) for 1 h at room temperature and endogenous peroxidase blocked with 0.5% hydrogen peroxidase (Sigma) in methanol for 30 min. Next, slides were incubated with the primary antibody rat anti-mouse B220 (Biolegend), anti-mouse F4/80 (Serotec AbD), and rat anti-mouse Cd49b (Biolegend) at 4°C overnight. The sections were then briefly washed and incubated with biotinylated secondary anti-rat IgG or IgM antibodies (Southern Biotech) for 30 min at room temperature. The secondary antibody was then visualized by incubating sections with fluorescein or Texas Red avidin D. Staining for CD3 was performed using the rabbit anti-mouse CD3 antibody (clone SP7; Vector laboratories) in conjunction with the Dako EnVision kit according to the manufacturer's guidelines. Staining for WNV was performed using antibody 7H2 (Bioreliance).

Administration of chemokine antagonists to mice. Chemokine antagonists to CCR2, CCR5, and CXCR3 were administered to SFV-infected mice. The CCR2 antagonist RS504393 (Tocris) was given to mice orally twice daily at a concentration of 5 mg/kg of body weight/day in 300 μl PBS with 6.6% dimethyl sulfoxide (DMSO) (29). This antagonist has been shown to be selective for CCR2 and does not interfere with ligand binding to CCR1, CCR3, or CXCR1 (30). The measured 50% inhibitory concentration (IC_{50}) is 105 nM. The CXCR3 antagonist, designated compound 21, was kindly provided by Amgen Inc. (California, USA). Compound 21 was injected subcutaneously (s.c.) once daily at a concentration of 10 mg/kg/day in 50% DMSO (Sigma), 25% polyethylene glycol (PEG) 400 (Sigma), and 25% sterile water (Qiagen) (31). Limited information is available regarding the specificity of this blocker, but it is reported to be selective for CXCR3 and to display an IC_{50} of 40 nM (32). The CCR5 antagonist D-Ala-peptide T-amide (DAPTA; Tocris) was administered to mice s.c. at a concentration of 1 mg/kg/day once daily (33, 34). This antagonist has been shown to be selective for CCR5 and does not inhibit ligand binding to CCR1 or CXCR4. It displays an IC_{50} of 55 pM (35). DAPTA displays a half-life of 30 to 60 min and a compartment half-life of 6 to 7 h (36). The treatment of mice with all the blockers started on PID 3 and was administered until PID 7 or until mice became ill. Mice infected with SFV A7(74) were euthanized on PID 7. Mock-treated mice were mock treated with vehicle control.

Statistical analysis. All data shown are expressed as means ± standard errors of the mean (SEM) unless stated otherwise. The D'Agostino and Pearson omnibus K2 or Shapiro-Wilks test was performed to test if data were normally distributed. The appropriate statistical test was performed for each data set using Prism 4 software (Graphpad) and is indicated in the figure legends. In brief, when appropriate, a one-way analysis of variance (ANOVA), Student's *t* test, Kruskal-Wallis test, or Mann-Whitney U test was performed. The survival analysis was performed using the log rank test. A *P* value of <0.05 was considered statistically significant.

RESULTS

Chemokines are upregulated in the CNS during SFV infection. Chemokines are essential for controlling the migration and positioning of leukocytes and are either expressed at low levels or completely absent in the healthy CNS. Accordingly, analysis of chemokines during encephalitis will provide important insights into the nature of leukocyte infiltration and will highlight possible interventionist points for therapy. Therefore, to examine chemokine expression during viral encephalitis, we initially utilized a tractable, and self-limiting, model of CNS viral infection involving the avirulent Semliki Forest virus strain A7(74). This virus was injected i.p. and, after an initially high titer of SFV in the blood (Fig. 1A), was cleared from the periphery and replicated to a high titer in the CNS (1.1×10^6 transcript copies of SFV E1 per 10^3 copies of TBP [Fig. 1B]). Histological analysis of brain sections demonstrated foci of SFV infection scattered throughout the brain, particularly around the hippocampus, thalamus, and striatum (Fig. 1C). SFV infection of the brain led to a rapid induction of tumor necrosis factor (TNF) transcripts and of interferon (IFN)-inducible genes from PID 3 onwards (Fig. 1D) that closely mirrored SFV titers within the brain. A cumulative increase in the panleukocyte marker, CD45 transcript, was also seen, suggesting leukocyte entry into the infected brain. Thus, this model of virus infection induces a consistent sequence of infection and cytokine production in the CNS.

To better understand the mechanisms that regulate leukocyte infiltration into the SFV-infected brain, we next measured CNS chemokine expression using TaqMan low-density arrays. SFV A7(74) infection triggered the expression of a key, but select, group of inflammatory chemokines (Fig. 1E and F), the expression of which lagged behind the early induction of TNF- and IFN-based responses. At the peak of viral infection on PID 7, inflammatory CC chemokine transcripts such as CCL2 and CCL5 increased more than 90-fold ($P < 0.01$), and CCL3, CCL4, CCL7, and CCL8 increased more than 30-fold ($P < 0.05$) compared to what was seen in healthy mouse brain (Fig. 1E). Importantly, not all inflammatory CC chemokines were upregulated, and no enhancement of CCL11 expression, for example, was seen. Within the inflammatory CXC chemokine family, induction followed the same temporal pattern as seen for the CC chemokines. By PID 7, CXCL9 and CXCL10 were the most upregulated chemokine transcripts at 300- and 400-fold upregulation, respectively (Fig. 1F). Modest induction of CXCL16 was also noted at later time points. CXCL1 expression levels were only minimally and not significantly upregulated compared to healthy control brains. Similar to CC chemokine expression levels, not all inflammatory CXC chemokines were upregulated, suggesting specificity to the chemokine expression. Chemokines such as CXCL12 or fractalkine (CX_3CL1) did not change their transcript levels in the brain during SFV infection compared to healthy mice (Fig. 1F). Thus, infected CNS tissues displayed early, robust expression of key inflammatory cytokines that preceded the expression of a select group of inflammatory chemokines.

To examine chemokine expression in the context of a virulent and highly pathogenic virus, we next examined the impact of infection with a lethal SFV strain, L10, on chemokine expression. SFV L10 infection of brain tissue induced a substantially more robust, comprehensive, and rapid production of chemokines than was seen with the A7(74) strain. Chemokines in L10-infected mouse brains were measured before (asymptomatic, on PID 4) and after the onset of neurological symptoms (symptomatic, between PID 5 and PID 6), when mice exhibited neurological signs typical of alphavirus-induced encephalitides (Fig. 1Gi and Gii) (3). The most upregulated chemokines in symptomatic mice were CCL2 and CXCL9 (>3,000-fold), followed by CCL7, CXCL2, and CXCL10 (>2,000-fold). While the expression pattern of CXC chemokines was somewhat similar for A7(74) and L10, the magnitude of upregulation was much higher in L10-infected brains, and additionally L10 induced the expression of CXCL1 and CXCL2, which were expressed only at low levels during A7(74) infection. Thus, inflammatory chemokines are highly upregulated in the brain during infection with SFV and therefore represent plausible therapeutic targets.

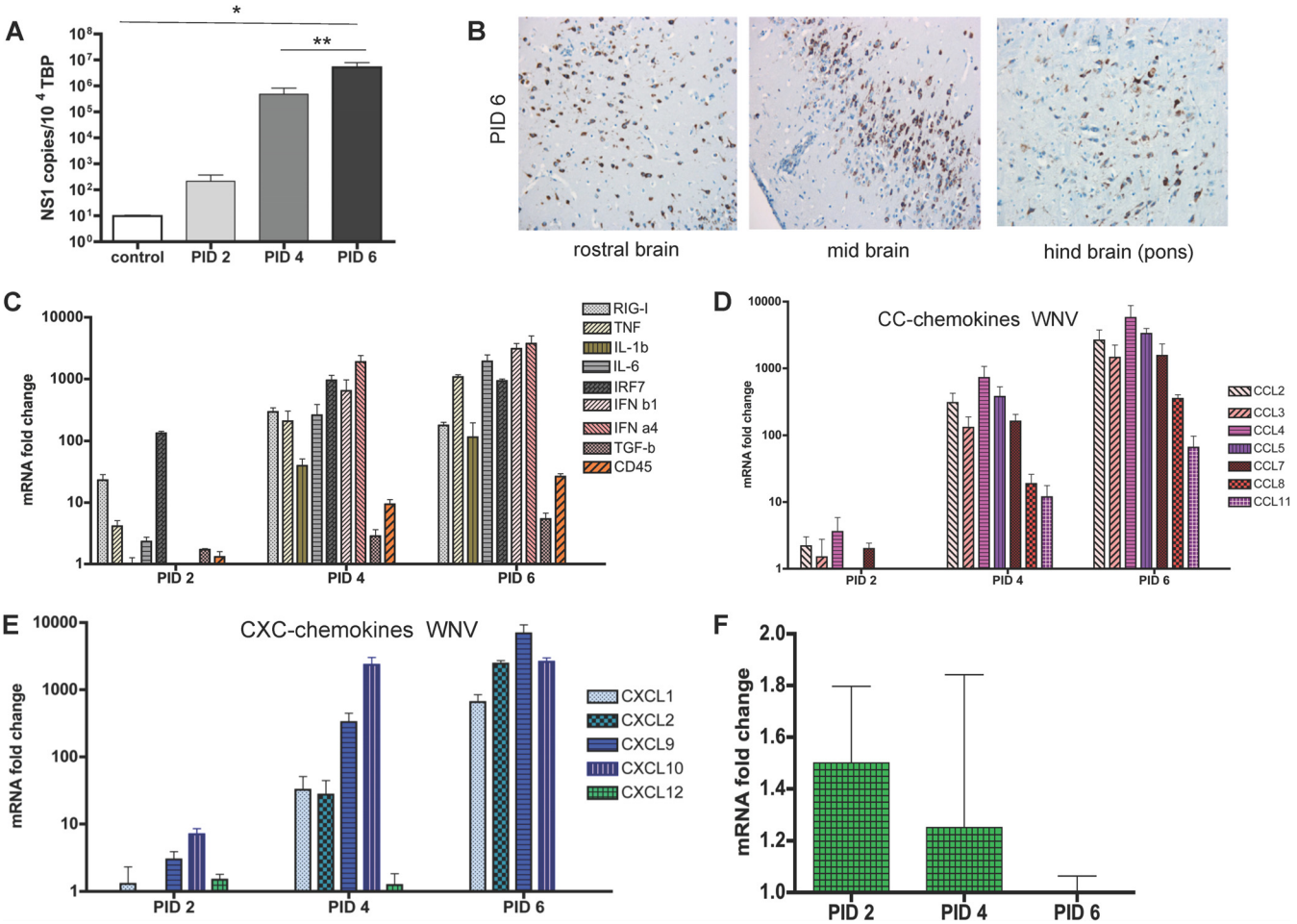

FIG 2 Inflammatory cytokine and chemokine responses to West Nile virus. (A) QPCR analysis of viral titers in the CNS of mice at the indicated time points following viral inoculation. Numbers of copies of the viral NS1 transcript are expressed per 10^3 copies of the housekeeping TBP gene (Kruskal-Wallis test with Dunn's posttest; *, $P < 0.05$; **, $P < 0.01$). (B) Immunostaining showing the sites of viral infection in mouse brains. Brown staining represents detection of WNV nonstructural protein NS1. Magnification, ×20. (C to F) TaqMan low-density array analysis of the expression of inflammatory cytokines, interferon response elements, and CD45 (C), inflammatory CC chemokines (D), CXC chemokines (E), and CXCL12 transcripts (F) in the brains of mice at the indicated time points after inoculation with West Nile virus. Data are expressed as fold changes in expression relative to healthy control mouse brains. Each sample was tested in triplicate with 4 to 5 mice per time point.

WNV infection induced the expression of many inflammatory chemokines in the brain. To investigate if CNS chemokine expression patterns during viral encephalitis are pathogen specific, we also defined expression following infection with the virulent WNV strain NY99. Following i.n. viral inoculation, all mice died by PID 6 to 7 and exhibited a high CNS viral titer (Fig. 2A), with virus scattered throughout the brain (Fig. 2B). WNV infection resulted in a more-rapid, broader-based, and higher-level induction of inflammatory cytokines than avirulent SFV A7(74), suggestive of a more aggressive CNS response to the virus (Fig. 2C). The response was, however, comparable to that seen with the virulent SFV L10. A rapid increase in CD45 transcript levels was also seen, suggesting leukocyte entry into the CNS. This occurred concomitantly with a rapid upregulation of both CC and CXC chemokines. Notably, and in contrast to the avirulent SFV strains, all chemokine transcripts assayed were substantially upregulated (>1,000-fold in some cases) in the brains, with the exception of CXCL12 (Fig. 2D and E). Interestingly, transcript levels for CXCL12 are not altered during the course of the encephalitis (Fig. 2F), although it is notable that a previous report indicated a specific reduction in expression of the CXCL12β isoform during WNV encephalitis (37). Importantly, the primer set used in our study does not discriminate between the α and β isoforms and therefore reports total CXCL12 expression. Thus, during WNV infection of the CNS, chemokines, cytokines, and interferon-stimulated genes were rapidly upregulated in an apparently broad and nonspecific manner.

Accumulation of NK cells, CD11b$^+$ myeloid cells, and B cells in response to CNS virus infection. To examine the association of the induced chemokines with leukocyte influx, we next used flow cytometry to determine the leukocyte subtypes accumulating in the SFV A7(74)-infected brain. As anticipated, healthy control mouse brains contained only a small number of leukocytes (CD45^{hi} cells). Following infection, CNS-infiltrating leukocytes were significantly increased from PID 5 onwards, and numbers peaked at PID 10 (Fig. 3Ai and Aii). In terms of CNS entry by specific leukocyte subtypes, the patterns that emerged were as follows.

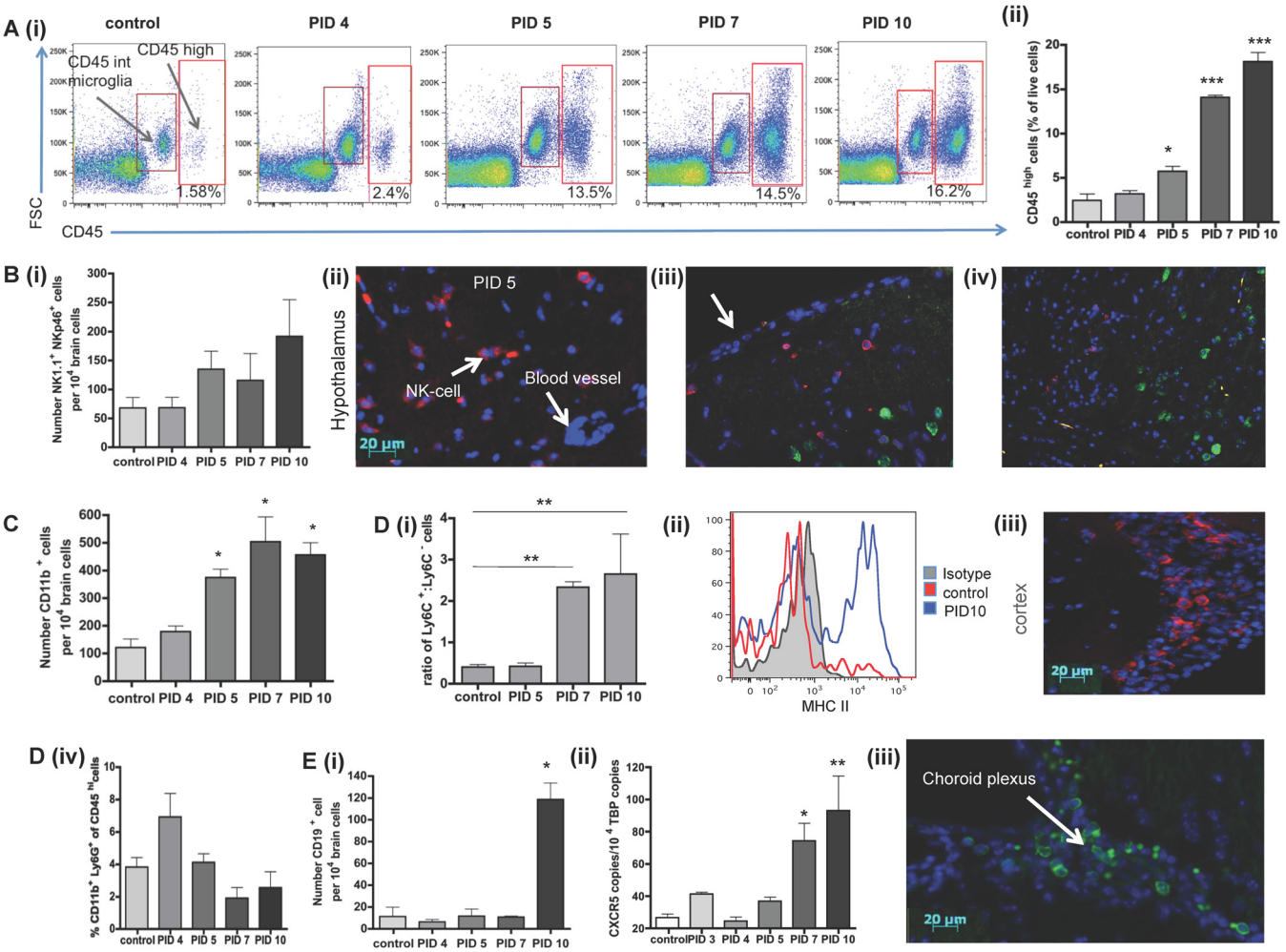

FIG 3 Analysis of the leukocyte content of virally infected brains. (A) Flow cytometric (i) and quantitative (% of live cells) (ii) analysis of the influx of $CD45^+$ leukocytes into the brains of control and infected mice at the indicated times points after inoculation with SFV A7 (74). Cells were gated on live cells, and doublet exclusion was performed. (B) Numbers of $NK1.1^+$ cells in the brain (i); images of histological analysis of the influx of NK cells into the hypothalamus of virally infected mice using the CD49b antibody (red) (ii), location of NK cells (CD49, red) and neurons (neuN, green) in the cortical region of the brain, with the meningeal surface indicated by the arrow (iii), and NK cells (CD49b, red) and SFV (nsp3, green) staining distal from each other in the brain (iv). (C) Numbers of $CD11b^+$ cells at the indicated time points following viral inoculation. (D) (i) Flow cytometric analysis of the ratio of $Ly6C^+$ and $Ly6C^-$ cells in SFV-infected and control brains. (ii) Measurement of the expression of MHC-II on infiltrating $Ly6C^+$ monocytic cells. (iii) Immunohistochemical analysis of the distribution of $F4/80^+$ macrophages in infected brains. (iv) Enumeration of $CD11b^+Ly6G^+$ neutrophils in the brains at the indicated time points following SFV infection. (E) (i) Numbers of $CD19^+$ cells of virally infected mice at the indicated time points following viral inoculation or in controls. (ii) Copy numbers of CXCR5 per 10^4 copies of TATA binding protein (TBP) by QPCR. (iii) Immunohistological analysis of the distribution of $B220^+$ B cells in virally infected brains. For all flow cytometric data, 5 to 10 pooled mouse brains per time point from 3 individual experiments were used. Significance was determined by the Kruskal-Wallis test with Dunn's posttest; *, $P < 0.05$, **, $P < 0.01$.

(i) Small numbers of NK cells ($NK1.1^+$ and $Nkp46^+$) entered the brain first with NK cell numbers peaking at PID 10 (Fig. 3Bi). Histological analysis of brain sections from infected mice showed that NK cells accumulated to high numbers (Fig. 3Bii) mainly in cortical areas of the brain (Fig. 3Biii) remote from viral foci (Fig. 3Biv).

(ii) Similarly, small numbers of $CD11b^+$ cells rapidly entered the CNS following viral infection. The number of $CD11b^+$ cells was significantly increased by PID 5 ($P < 0.05$), and levels were maximal at PID 7 ($P < 0.05$) (Fig. 3C). Following "gating out" of $Ly6G^+$ cells to remove neutrophils from the analysis [neutrophils were rare in the brain and did not change in number over the course of the SFV A7(74) infection (Fig. 3Div)]. $CD11b^+$ cells were further defined as $Ly6C^+$ or $Ly6C^-$. Between PID 5 and PID 7, we observed a significant shift from $CD11b^+Ly6C^-$ cells to $CD11b^+Ly6C^{hi}$ monocytes/macrophages (Fig. 3Di). Based on previous studies, $Ly6C^{hi}$ cells are referred to as "inflammatory monocytes" (38). The $Ly6C^{hi}$ cell fraction was further analyzed for the expression of MHC-II molecules. A shift from MHC-II-negative to MHC-II-positive cells could be observed on PID 7 and 10 (Fig. 3Dii). Using immunohistochemistry, only few $F4/80^+$ cells could be detected in SFV A7(74)-infected murine brain samples. Those cells were located mainly in the meninges that line the cortex and the lateral sulcus (Fig. 3Diii). Together, based on immunohistochemistry and also FACS data (not shown), only few macrophages (defined as being $F4/80^+$ and $MHCII^+$) are detectable in

the SFV-infected CNS, and this suggests that most of the $CD11b^+$ cells were monocytes rather than macrophages.

(iii) Substantial numbers of $CD19^+$ B cells appeared in the CNS during later stages of infection (Fig. 3Ei). Analysis by immunohistochemistry and qPCR (using CXCR5 expression as a marker for B cell infiltration) showed that B cells accumulated in the brain by PID 10 or later (Fig. 3Eii and Eiii). This suggests that B cells infiltrate the brain toward the end of the acute phase of the infection. B cells were localized mainly around the lateral ventricles and along the lateral sulcus and were not detectable in the brain parenchyma or any other areas of the brain (Fig. 3Eiii).

(iv) In contrast to the cells mentioned above, neutrophils, which are $CD11b^+$ $Ly6G^+$ $Ly6C^-$, were not detected in the brain by either flow cytometry or immunohistochemistry at any time point (data not shown).

Overall, these data demonstrate that SFV A7(74) infection induces the early infiltration of NK cells, followed by $CD11b^+$ myeloid leukocytes and then B cells into the CNS.

$CD3^+$ T cells accumulate in the brain from PID 7 onwards and infiltrate the brain parenchyma. Given the strong induction of CXCL9 and CXCL10, both CXCR3 ligands, following viral infection of the brain, it is not surprising that the most prominent leukocyte subtype entering the CNS between PID 7 and PID 10 was $CD3^+$ T cells (Fig. 4Ai and Aii). Proportions of $CD3^+$ T cells indicated that 20% of $CD45^{hi}$ cells are T cells, and this percentage increased significantly by PID 7 and PID 10 to almost 60%. T cells were detected in SFV brain sections localized in deep layers of the parenchyma throughout the brain (Fig. 4B). Many of the T cells accumulated around blood vessels, forming perivascular cuffing, and in the meninges (Fig. 4B) or colocalized with B cells around the lateral ventricle and lateral sulcus (Fig. 4C). Distinct $CD4^+$ and $CD8^+$ T-cell fractions were detected using flow cytometry (Fig. 4D). In healthy control brains, the ratio of $CD8^+$ and $CD4^+$ within the $CD3^+$ T-cell population was equal to 1. However, this ratio changed over the course of infection in favor of $CD8^+$ cells, which were significantly ($P < 0.001$) more abundant in the CNS on PID 7 and 10 than healthy control brains (Fig. 4D). The ratio of $CD4^+$ T cells was similar to that in control brains over the time course of infection. Almost 80% of all infiltrating $CD3^+$ T cells were effector T cells showing a high expression of CD44 and low expression of L-selectin (CD62L), and the number of effector T cells was significantly increased by PID 7 and 10 (Fig. 4E). Further phenotyping of infiltrating T cells demonstrated, in keeping with high expression of CXCL9 and CXCL10, that the majority expressed CXCR3 (Fig. 4G). The expression of the chemokine receptor CCR5, often found on inflammatory cells, was also detectable on T cells at PID 7 and 10, and the number was significantly increased at these time points postinfection ($P < 0.05$ and $P < 0.01$, respectively) (Fig. 4F). Thus, T cells, predominantly $CD8^+$, expressing CD44, CXCR3, and CCR5 accumulate in the brain on, or after, PID 7 and are localized throughout the brain parenchyma.

CCR5 blockade reduces leukocyte accumulation in the brains of infected mice. CCR5 has been reported to be important for the migration of monocytes, macrophages, T cells, and NK cells (39). Since CCR5 ligands were expressed in the SFV-infected brain, we examined the role of CCR5 in leukocyte accumulation during SFV-dependent encephalitis. Blockade with the CCR5 blocker DAPTA resulted in a modest, but not significant, reduction in $CD45^+$ leukocyte recruitment into the CNS (Fig. 5Ai). Importantly, however, the number and percentage of $CCR5^+$ leukocytes were significantly reduced ($P < 0.01$) in treated mice compared to mock-treated mice, confirming the effectiveness of the small-molecule antagonist (Fig. 5Aii). The numbers of individual leukocyte subtypes were reduced by CCR5 blockade, including T cells, myeloid cells, and NK cells (Fig. 5B to D). Notably, none of these reductions were statistically significant ($P > 0.05$). Importantly, CCR5 blockade had no effect on viral titer (Fig. 5E). Thus, CCR5 plays a minor role in leukocyte entry into the CNS, but this does not lead to alterations in viral titer.

CCR2 blockade significantly reduced monocyte/macrophage infiltration of infected mouse brains. CCR2 ligands CCL2 and CCL7 were also strongly upregulated during viral encephalitis in both SFV and WNV studies, so we next evaluated the impact of blocking this receptor during SFV infection. As CCR2 is strongly expressed by monocytes, but less so than NK and T cells, we hypothesized that blocking CCR2 would lead to a selective reduction of monocyte infiltration. Since infection with some viruses such as WNV can dramatically alter the levels of circulating monocytes (40, 41), we first sought to define the kinetics of monocyte mobilization into the blood in response to SFV infection. During the first 48 h of infection with SFV, the numbers of $CD11b^+$ cells (Fig. 6Ai) and $CCR2^+$ monocytes (Fig. 6Aii) were significantly increased ($P < 0.05$) in the blood, following which numbers slowly decreased, concomitantly with reduced serum viremia. The proportion of $CD11b^+$ cells decreased significantly after 48 h postinfection (Fig. 6Ai).

To examine the involvement of CCR2 in leukocyte accumulation in the brain during viral encephalitis, the CCR2 blocker RS504393 was administered to SFV-infected mice and leukocyte accumulation was assessed by flow cytometry and compared to that in untreated mice. Mice were first infected with SFV A7(74) and then treated with CCR2 blocker, or vehicle control, for 4 days starting on PID 3 and ending on PID 7. The accumulation of $CD45^{hi}$ leukocytes was significantly ($P < 0.001$) reduced by up to 57% in mice treated with the CCR2 blocker (Fig. 6Bi and Bii). To further confirm roles for CCR2 in leukocyte accumulation in infected CNS, we also used $CCR2^{-/-}$ mice, in which leukocyte infiltration was markedly reduced to a level similar to that observed in mice treated with RS504393 (Fig. 6Bii). Next, we analyzed the number of $CD11b^+$ cells in untreated, blocker-treated, and $CCR2^{-/-}$ mice. $CD11b^+$ cell numbers were significantly reduced in treated and $CCR2^{-/-}$ mice (for both, $P < 0.01$) and the proportion and number of double positive $CD11b^+CCR2^+$ monocytes were reduced to almost zero (Fig. 6Ci, Cii, and Ciii). While CCR2 is predominantly involved in the migration of myeloid cells, it is also expressed on other cell types. We therefore examined the impact of CCR2 blockade on the recruitment of other leukocyte subtypes into the infected CNS. These results demonstrated that both $CD3^+$ T-cell and NK cell numbers were significantly ($P < 0.05$) reduced after genetic or pharmacological blockade of CCR2 (Fig. 6Di and ii). Despite inducing a significant and robust reduction in leukocyte entry, CCR2 blockade was not associated with altered SFV brain titers (Fig. 6E).

In a previous study using WNV, it was reported that CCR2 plays an important role in the egress of monocytes from the bone marrow and return of monocytes from the blood to the bone marrow (41). Therefore, we wanted to examine if the reduction of monocytes in the CNS of SFV-infected, and CCR2 blocker-treated, mice was due to monocytopenia. We found that the pro-

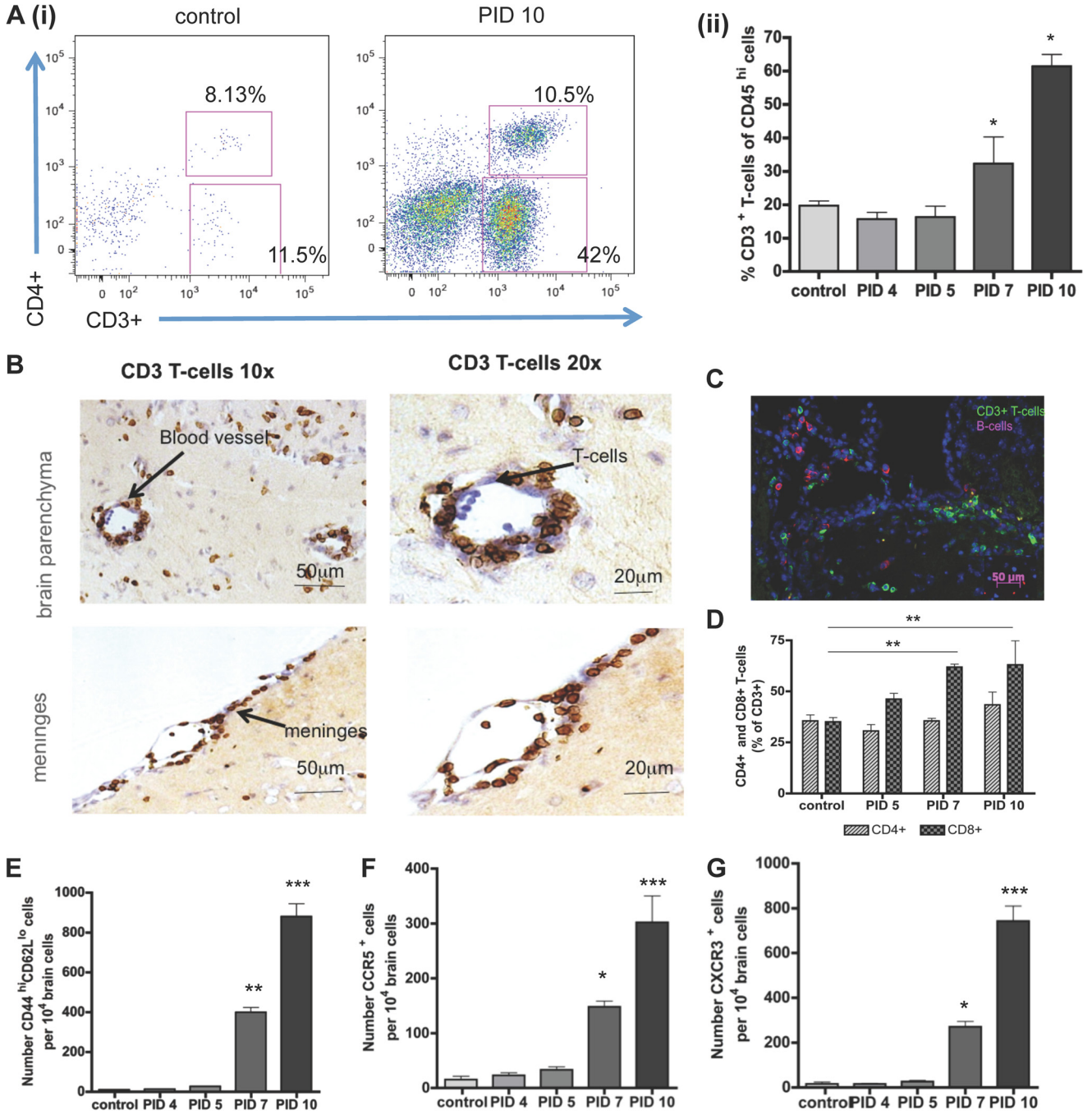

FIG 4 Analysis of the infiltration of virally infected brains by T cells. (A) (i) Demonstration of the marked influx of T cells into control and virally infected mouse brains at 10 days following viral inoculation. (ii) Proportion of $CD3^+$ T cells in control and virally infected brains at the indicated time points. (B) Immunohistological staining demonstrating the perivascular and meningeal localization of infiltrating T cells in the brains of virally infected mice. Magnification, ×10 and ×20. (C) Immunohistological localization of T cells and small numbers of B cells in the virally infected brain. (D) Quantitation of the relevant representation of $CD4^+$ and $CD8^+$ T cells at the indicated time points following viral inoculation (Expressed as the percentage of the overall $CD3^+$ T-cell population). (E to G) Numbers of $CD44^+CD62L^+$ cells (E), $CCR5^+$ cells (F), and $CXCR3^+$ cells (G) per 10^4 brain cells in control and infected brain samples at the indicated time points following viral inoculation. For all flow cytometric data, 5 to 10 pooled mouse brains per time point from 3 individual experiments were used. Significance was determined by the Kruskal-Wallis test with Dunn's posttest (A and E), one-way ANOVA with Tukey's posttest (F and G), and two-way ANOVA with Bonferroni's posttest (D); *, $P < 0.05$; **, $P < 0.01$; ***, $P < 0.001$.

portion of circulating monocytes, of both $CD11b^+Ly6C^+CCR2^+$ and $CD11b^+Ly6C^-$ phenotypes, was not significantly reduced during the treatment with the CCR2 blocker (Fig. 6Fi and Fii). Thus, CCR2 plays a critical role in the accumulation of monocytes/macrophages and T cells in the brain but has no significant effect on viral titer.

The chemokine receptor CXCR3 orchestrates the accumulation of substantial numbers of leukocytes. Since the CXCR3 li-

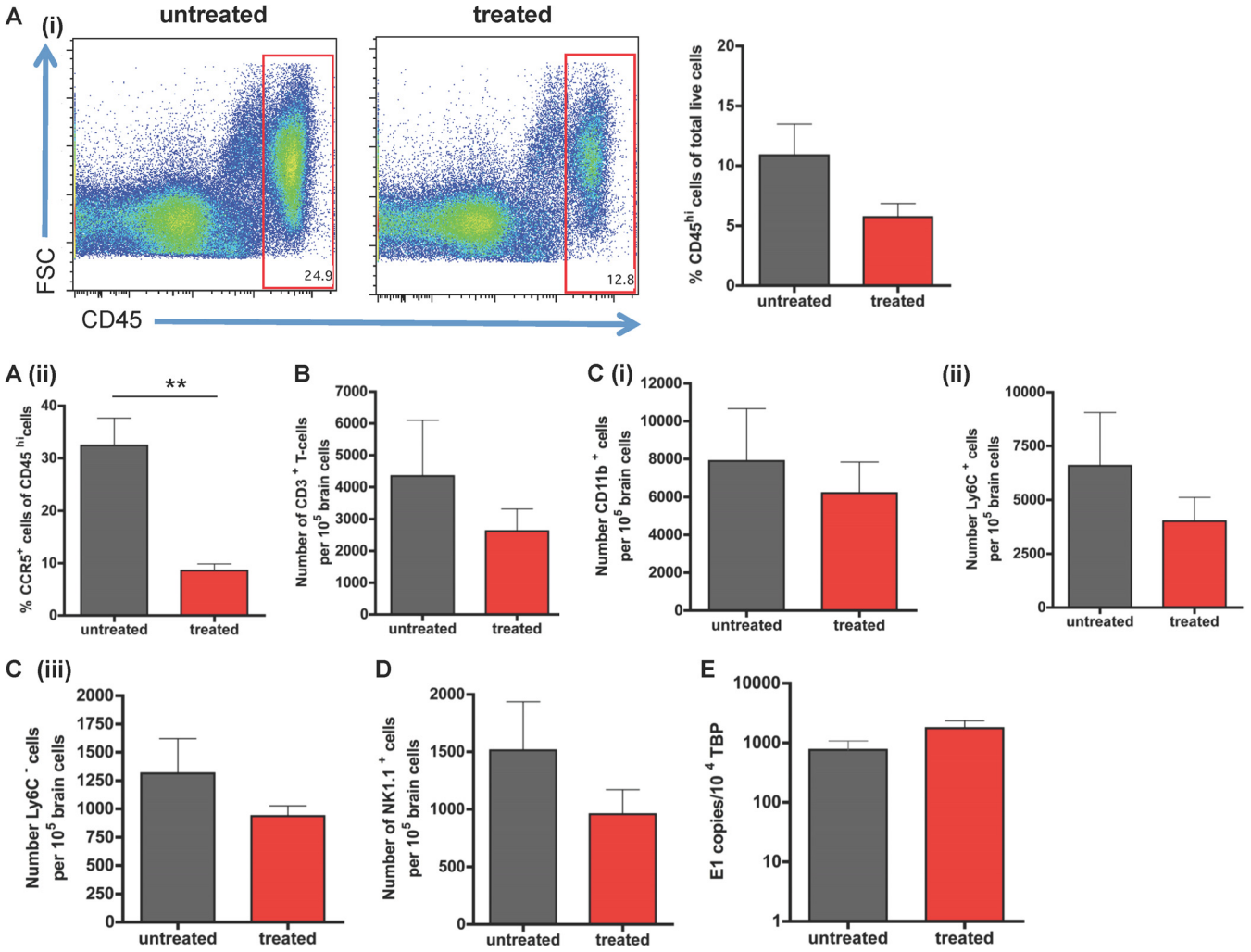

FIG 5 Effects of CCR5 blockade on viral encephalitis. (A) (i) Flow cytometric analysis demonstrating the reduction in total $CD45^+$ cell counts in virally infected SFV brains of CCR5 blocker-treated and untreated mice. This difference was only modest and not statistically significant. (ii) Quantitative flow cytometric data demonstrating a significant reduction in the percentage of $CCR5^+$ leukocytes in the virally infected brains of CCR5 blocker-treated mice. (B and C) Numbers of $CD3^+$ T cells (B), $CD11b^+$ cells (Ci), $Ly6C^+$ (Cii), and $Ly6C^-$ cells (Ciii) per 10^5 brain cells in SFV-infected mice treated with either CCR5 blocker or vehicle control. Numbers were obtained by flow cytometric analysis. (D) Quantitation of flow cytometric data demonstrating the decrease in NK cell accumulation in SFV-infected mice treated with the CCR5 blocker compared to that in mock-treated mice. (E) QPCR analysis of viral titers demonstrating no significant effect of CCR5 blockade on overall viral titers in infected brains. All results were not statistically significant for all experiments; $n = 4$ to 6 pooled mouse brains from 2 individual experiments (Student's t test; $P > 0.05$).

gands CXCL9 and CXCL10 were the most highly upregulated chemokines in the CNS during viral infection, we finally examined the consequence of CXCR3 blockade on T-cell accumulation in the CNS. To this end, we obtained a previously characterized CXCR3 blocker referred to as "compound 21" (31). The blocker, or vehicle control, was administered to SFV A7(74)-infected mice from PID 3 until PID 7, when mice were euthanized and brains harvested for flow cytometric evaluation. The accumulation of $CD45^{hi}$ leukocytes was dramatically reduced ($P < 0.01$) in the mice treated with the CXCR3 blocker (Fig. 7Ai and Aii). Within the $CD45^{hi}$ leukocyte population in the CNS, the number of $CD3^+$ T cells was substantially and significantly ($P < 0.01$) reduced compared to that in the untreated SFV-infected control groups (Fig. 7Bi). Within the reduced T-cell population, compound 21 significantly reduced the influx of both the $CD4^+$ and $CD8^+$ T-cell populations into the CNS, although a more profound reduction in $CD8^+$ T-cell numbers was apparent (Fig. 7Bii). The number of CXCR3-expressing cells was also markedly reduced (Fig. 7C). To investigate the impact of compound 21 on recruitment of other leukocyte subtypes, we analyzed the number of $CD11b^+$ cells and NK cells in the brains of both treated and untreated mice. The overall number of $CD45^{hi}$ $CD11b^+$ cells in the brains of treated mice was also dramatically reduced, but statistical significance could not be calculated (Fig. 7Di). No significant differences in the numbers of NK cells were detected (Fig. 7Dii). Interestingly, despite the significant reduction in leukocyte entry, the number of SFV E1 transcripts in the brain was unaffected by CXCR3 blockade (Fig. 7E).

Chemokine receptor blockade is therapeutically efficacious in mice treated with virulent SFV. Finally, we examined the impact of chemokine receptor blockade on disease outcome using the virulent SFV strain L10. We infected mice with the virulent

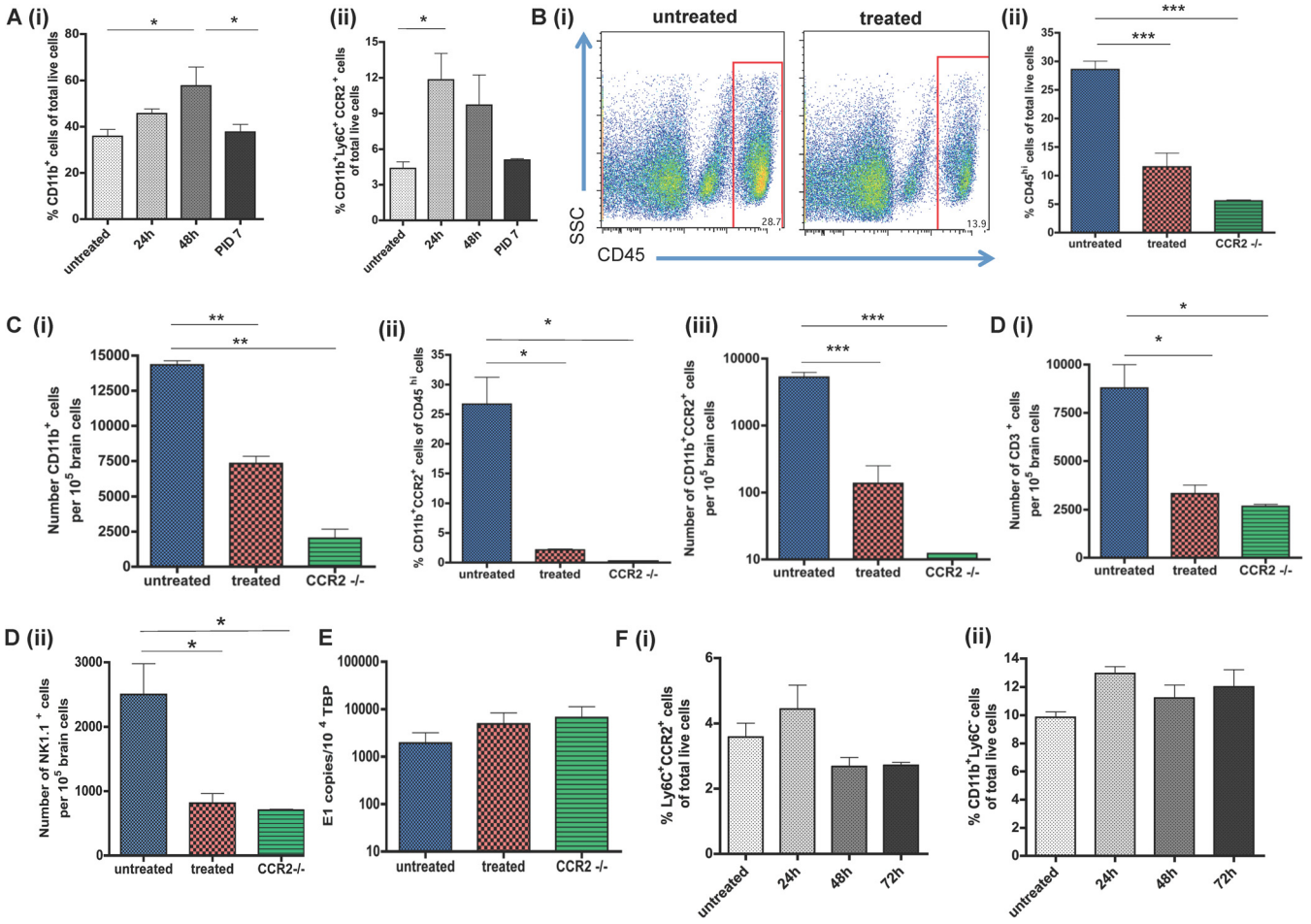

FIG 6 Effects of CCR2 blockade on viral encephalitis. (A) Number of $CD11b^+$ cells (i) and CCR2 $^+$ monocytes (ii) in the blood at the indicated time points following viral inoculation with SFV A7 (74). Both results are expressed as percentages of total cells counted. (B) (i) Decrease in $CD45^{hi}$ cell numbers at PID 7 in mice treated with the CCR2 blocker or in $CCR2^{-/-}$ mice. (ii) Quantitation of the differences in $CD45^+$ cell accumulation at PID 7 in the brains of mice treated with the CCR2 blocker or CCR2 knockout (KO) mice compared to untreated wild-type mice. (C) (i) Accumulation of $CD11b^+$ cells in the brains of virally infected mice at PID 7. Proportions (ii) and numbers (iii) of $CCR2^+CD11b^+$ cells in the brains of untreated wild-type, CCR2 blocker-treated wild-type, and CCR2-deficient mice at PID 7. (D) Accumulation of $CD3^+$ T cells (i) and NK cells (ii) in the brains of virally infected mice at PID 7. (E) QPCR analysis of viral titers in the brains of SFV-infected mice at PID 7. Data are expressed as numbers of copies of the viral E1 transcript per 10^4 copies of the housekeeping TBP gene. (F) Percentages of circulating $CCR2^+$ monocytes (i) and $Ly6C^+$ cells (ii) in the blood of mice treated with the CCR2 blocker at the indicated time points. All data represent at least 2 replicate experiments and were acquired by flow cytometry ($n = 4$ to 7 pooled mouse brains per time point) except for data in panel E, which were acquired by QPCR ($n = 5$ mice per time point). Significance was determined by the Kruskal-Wallis test with Dunn's posttest (A) and one-way ANOVA (B to F); *, $P < 0.05$; ***, $P < 0.001$.

strain L10 and treated mice with the appropriate antagonists starting on PID 3. Neither CCR2 nor CCR5 blockade had any significant effect on survival in this model (Fig. 8A and B), suggesting that these receptors are not individually crucial to the encephalitic process. Given its profound effect on leukocyte recruitment, we next examined the effect of compound 21 on disease outcome. Despite its ability to significantly reduce leukocyte entry into the CNS during infection with SFV A7(74) (Fig. 7), we found no survival benefit in L10-infected mice treated with the CXCR3 antagonist (Fig. 8C).

To examine the possible impact of coblocking the 2 receptors identified as being the most active in the encephalitic process, CXCR3 and CCR2, we next treated L10-infected mice with blockers for both of these receptors. Again, both blockers were administered to mice starting on PID 3. Our results show that mice treated with both blockers had a significant survival advantage compared to control mice that were mock treated with vehicle control (Fig. 8D). Coblockade of CCR2 and CXCR3 results in a reduction in leukocyte accumulation similar in magnitude to that seen with CXCR3 blockade alone (data not shown). However, and in contrast to single blockade for CCR2 or CXCR3, coblockade of the two receptors resulted in a profound and significant reduction in viral titers in the brains of infected mice (Fig. 8E). This was associated with reduced transcript levels of key inflammatory mediators, including CXCL2 and TNF, but with no alterations in expression of the marker of astrocyte activation glial fibrillary acidic protein (GFAP) (Fig. 8F). This, along with the elevated expression of inducible nitric oxide synthase (iNOS), suggests that recruited leukocytes rather than resident astrocytes are driving the inflammatory response in the mice in the absence of receptor blockers. Thus, these data suggest that an interventionist strategy aimed at blocking CCR2, CCR5, or CXCR3 function alone

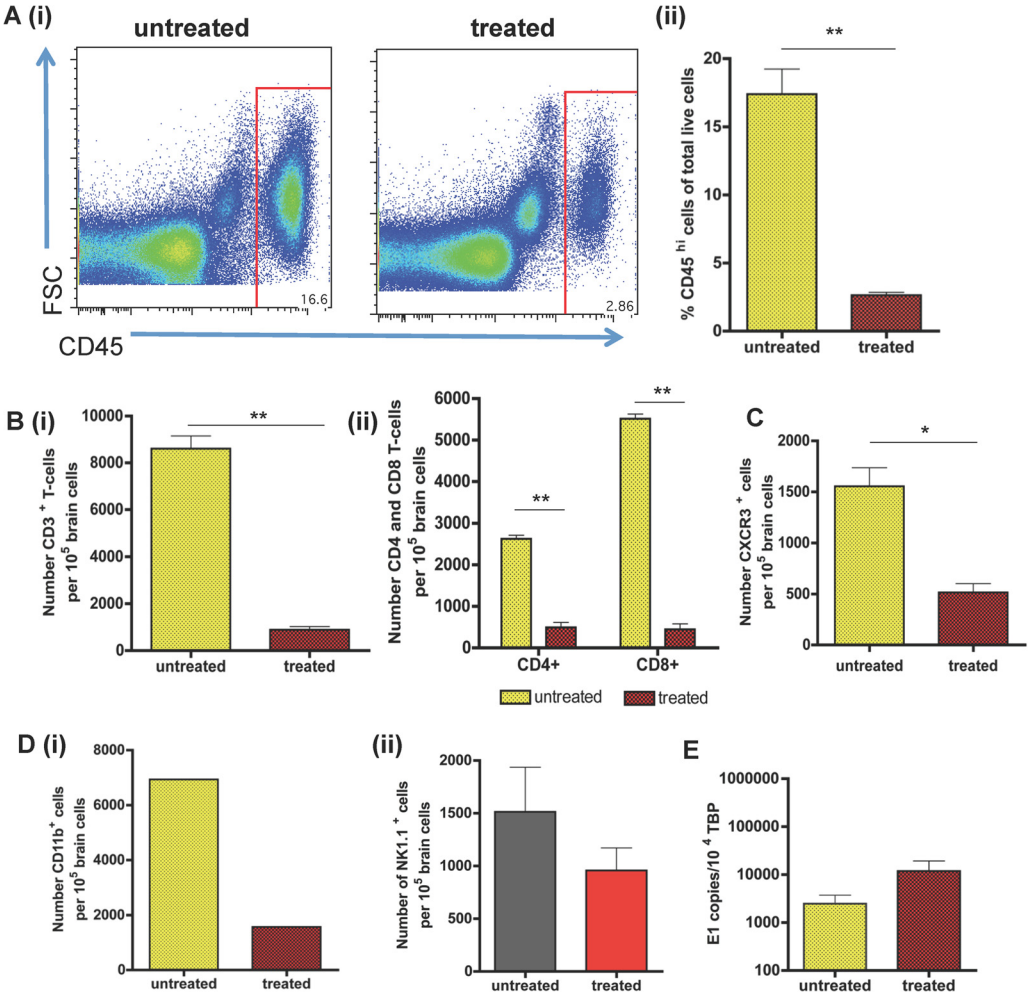

FIG 7 Effects of CXCR3 blockade on viral encephalitis. (A) Flow cytometric (i) and quantitative (ii) analysis of the impact of CXCR3 blockade on $CD45^+$ leukocyte accumulation at PID 7 in the brains of SFV A7 (74)-infected mice. (B) (i) Quantitative analysis of the effects of CXCR3 blockade on the accumulation of T cells at PID 7. (ii) Numbers of $CD4^+$ and $CD8^+$ T cells in the brains of CXCR3 blocker-treated mice at PID 7. (C and D) Quantitative analysis of the effects of CXCR3 blockade on the recruitment, at PID 7, of $CXCR3^+$ cells (C) and $CD11b^+$ (Di) and NK cells (Dii) into the CNS. (E) QPCR analysis of the effects of CXCR3 blockade on viral titers in the brains of virally infected mice at PID 7. Each sample was tested in triplicate with 5 mice per time point. Data are from 5 to 8 pooled mouse brains (A to D) or 4 mice per group (E) from 1 or 2 individual experiments. Cell numbers presented here are per 10^5 brain cells. Student's *t* test: *, $P < 0.05$; **, $P < 0.01$.

during virulent infection was ineffective at ameliorating disease but that simultaneous treatment with blockers for both CXCR3 and CCR2 led to a better disease outcome, indicating that leukocyte infiltration is associated with more-severe pathology during viral encephalitis. These data further highlight the potential use of chemokine receptor blockers in the treatment of viral encephalitis.

DISCUSSION

Leukocyte influx into the brain is a defining feature of viral encephalitis. It has long been assumed that leukocyte infiltration into the CNS is critical to clear virus and aid recovery. Alternatively, infiltrating leukocytes may paradoxically contribute to a more severe outcome that results from the destruction of neuronal cells. Chemokines are pivotal regulators of leukocyte trafficking (7, 9). In the context of viral encephalitis, it is not clear which chemokines are important for the attraction of leukocytes into the CNS and what role they play during viral infection of the brain, or indeed what impact this has on encephalitis-associated morbidity and mortality. The purpose of the present study was to use murine models of viral encephalitis to rigorously define chemokine involvement in leukocyte recruitment to the encephalitic brain. The secondary aim of the study was to examine the possibility of using interventionist strategies against identified chemokine receptors to suppress CNS leukocyte recruitment and modulate host immune responses, which in excess may otherwise contribute to virus-induced damage and mortality. Using these approaches, we have identified CXCR3, CCR2, and CCR5 as being key instigators of CNS inflammation that coordinate leukocyte trafficking to the brain during infection. We have used virulent and avirulent strains of SFV and WNV as models for viral encephalitis. Our data show that the chemokine expression patterns during viral encephalitis are similar regardless of the pathogen used, although more-virulent viral strains were associated with more-rapid and -comprehensive induction of inflammatory cytokines and chemokines. Thus, our findings demonstrate that a similar chemokine expres-

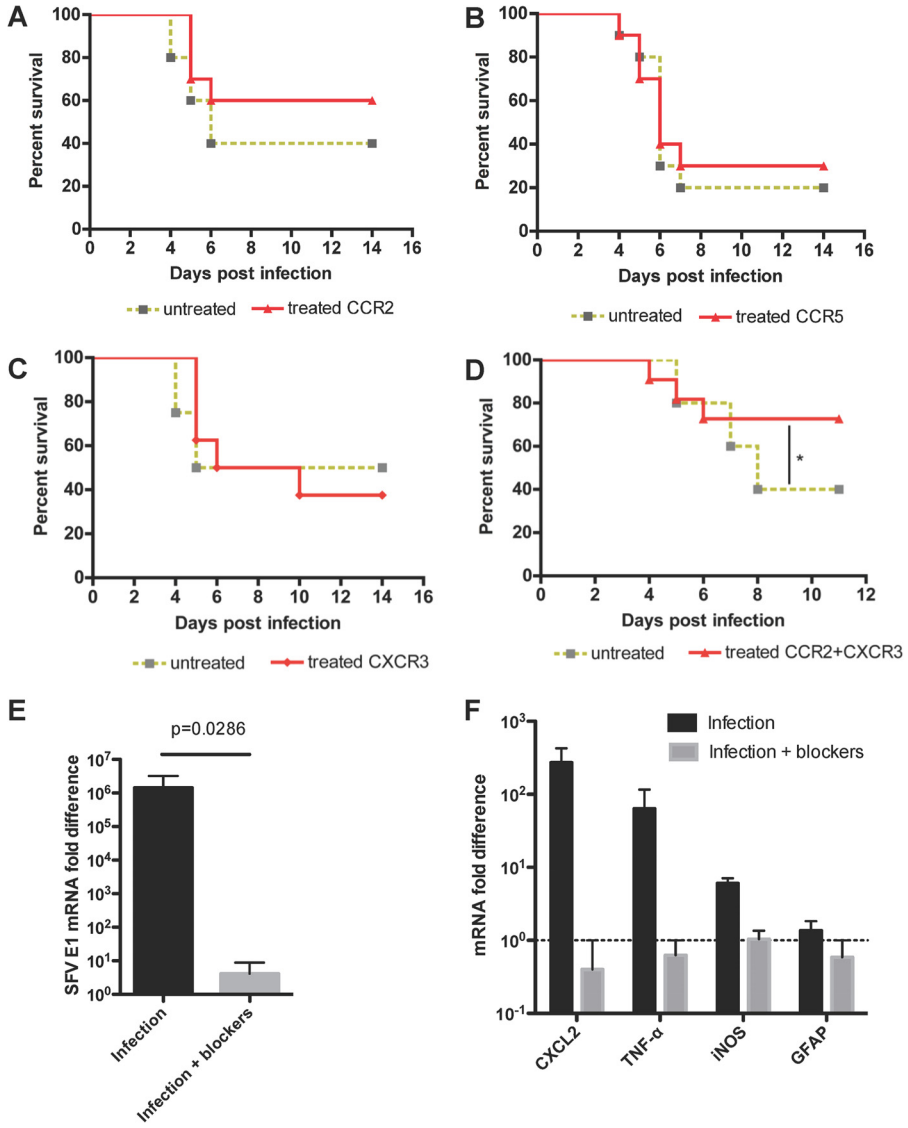

FIG 8 The effects of CXCR3 and CCR2 blockade on survival following inoculation with the virulent SFV strain L10. (A, B, C) Survival curves showing no effect of CCR2 (A), CCR5 (B), or CXCR3 (C) blockade on their own on survival of mice following inoculation with strain L10 of SFV. (D) Survival curves showing a significant difference of survival in untreated and CCR2- and CXCR3-treated wild-type mice (log rank test: *, $P < 0.05$; $n = 10$ mice per treatment group). (E) Coblockade of CCR2 and CXCR3 (infection + blockers) is associated with a significant reduction (one-tailed Mann-Whitney U test) in viral titers in the mouse brains compared to virus-treated mice receiving vehicle (infection). Viral titers are expressed as fold changes relative to expression in one of the blocker-treated brain samples. (F) Coblockade of CCR2 and CXCR3 (gray bars) is associated with reduced levels of transcripts for CXCL2, TNF, and iNOS but unaltered expression of GFAP compared to vehicle-treated infected mice. Transcript levels are expressed as fold changes as described for panel E.

sion pattern during viral encephalitis is evident regardless of the pathogen. Similar, but more limited, observations have been made for a number of viruses that cause encephalitis, including herpes simplex virus 1 (42), tick-borne encephalitis virus (43), and lyssaviruses (44). Based on our FACS data, we have demonstrated that mostly $CD8^+$ T cells and monocytes infiltrate the brain during SFV infection. Our result is in agreement with studies using WNV or mouse hepatitis virus (MHV) as a model of infection. Lim et al. have shown that many T cells and monocytes accumulate in the brain during WNV infection, in which they exert antiviral functions and reduce mortality. During MHV infection, similar observations were made and T-cell- or monocyte-deficient mice exhibited reduced survival (45–47).

We have demonstrated that blocking chemokine receptors with specific antagonists leads to a reduction in the numbers of leukocytes infiltrating the brain during infection with SFV. Given the high CXCL9 and CXCL10 transcript levels in the brain and large numbers of infiltrating $CD3^+$ T cells, we wanted to test if the CXCR3 antagonist, compound 21 (31), was able to decrease T-cell trafficking to the brain. We demonstrated that compound 21 was highly effective at blocking T-cell entry. Within the $CD3^+$ T-cell population, the numbers of $CD4^+$ and $CD8^+$ T cells were markedly reduced ($P < 0.01$) compared to those in untreated control mouse brains, and the extent of $CD8^+$ T-cell infiltration was particularly affected by blockade with compound 21. This corresponds with results obtained from studies with WNV, in which CXCR3-deficient mice exhibited a significant decrease in $CD8^+$ T-cell infiltration within WNV-infected mouse brains (17, 48).

The CCR2 ligand CCL2 was also strongly upregulated by both SFV and WNV infections in the brain. We have demonstrated in our study that blocking CCR2 with the antagonist RS504393 results in a significant decrease in monocyte accumulation in wild-type (WT) brains similar to that seen in CCR2-deficient mouse brains. Previous work with WNV, using CCR2 null mice, has suggested that this receptor plays a critical role only in monocyte egress from the bone marrow but also that it is otherwise dispensable for CNS entry (41). Importantly, we found that a temporary blockade of CCR2 did not result in a decrease in circulating monocytes but did block their CNS entry, suggesting that leukocytes do use this chemokine axis to enter the virus-infected CNS and that this is not an indirect consequence of monocytopenia. It is also worth noting that recent results from studies on "reporter mice" suggest that both astrocytes and resident microglia do not express CCR2, further supporting an effect of the pharmacological blocker in cellular recruitment to the brain rather than activation of resident $CCR2^+$ CNS cells (49).

Interestingly, for both CXCR3 blockade and CCR2 blockade, leukocytes that are not known to express these receptors were also reduced in number and proportion in the SFV-infected brain. Accordingly, CXCR3 blockade led to a substantial decrease in monocytes, while CCR2 blockade led to a reduction in T-cell numbers. This suggests that recruited leukocytes trigger the recruitment of other leukocyte subsets that respond to distinct chemotactic cues. Recruited leukocytes may do this either directly by synthesizing chemokine themselves or indirectly by inducing chemokine expression in resident neural cells, perhaps through the productions of cytokines, as has been suggested to occur during LCMV infection (50).

Previous studies have shown that both $CD4^+$ and $CD8^+$ T cells are dispensable for the clearance of CNS alphavirus in the presence of neutralizing IgG and that depletion of $CD8^+$ or $CD4^+$ T cells has been shown to be advantageous in reducing the extent of virus-induced inflammatory demyelination (51–54). Here, we demonstrate that in addition to T-cell depletion, selectively blocking T-cell and monocyte CNS influx through the use of chemokine receptor antagonists does not affect virus titers and instead promotes survival to an otherwise overwhelming encephalitis.

CCR5 blockade also led to a reduction in leukocyte numbers in the brain, but the reduction was less profound than that seen with CCR2 and CXCR3. We conclude that during SFV infection, CCR5 seems to play a minor role in viral pathogenesis. This finding is in contrast to studies using WNV as a model of infection (19). During WNV infection, it was shown that CCR5 plays a pivotal role in neuropathology (18, 55). CCR5-deficient mice displayed more-severe neurological symptoms and died earlier than WT mice. Furthermore, it was also observed that humans with the nonfunctional Δ32 CCR5 mutation (56) are more susceptible to developing severe neurological symptoms following WNV infection (18, 57).

Through the use of chemokine receptor blockers, we define in this study a chemokine hierarchy active during alphavirus-induced encephalitis. Interfering with the CXCR3 axis leads to the greatest reduction of leukocyte entry into the CNS. The antagonism of CCR2 and CCR5 also led to the reduction of leukocyte entry in response to SFV infection but to a lesser extent than what was seen with the CXCR3 blockade. Importantly, none of the receptor antagonists alone had a significant impact on viral titers, so the reduction in leukocyte recruitment is a direct result of receptor blockade and not a result of direct or indirect virus inhibition by the antagonists. Importantly, and in contrast to single-receptor blockade, simultaneous blockade of CXCR3 and CCR2 significantly reduced viral titers in the brains of infected mice and ameliorated pathology. This was associated with reduced inflammation in the brains of receptor blocker-treated mice, and we propose that the lower levels of leukocyte-induced damage, particularly at the blood-brain barrier, may limit viral entry into the brains and lead to enhanced survival. However, we cannot discount a contribution of reduced leukocyte-associated encephalitis to the therapeutic effects of these receptor blockers. It is worth mentioning that the ability of CXCR3 blockers to contribute to the amelioration of encephalitis is at odds with previous reports implicating CXCR3 in the recruitment of antiviral T cells to the encephalitic brain (17). It is possible that this discrepancy results from the use of blockers in wild-type mice in our study compared to the use of full CXCR3-deficient mice in the earlier study.

Overall, our study raises the possibility of using selective chemokine receptor blockers as therapeutic targets for the treatment of viral encephalitis, although it is likely that such blocking agents will need to be used in combination to overcome the apparent redundancy of chemokine-receptor interactions (58, 59).

ACKNOWLEDGMENTS

This study was supported by grants from the Wellcome Trust and the Medical Research Council. Work in G.J.G.'s laboratory is funded by a Medical Research Council Programme Grant and by a Wellcome Trust Senior Investigator Award.

We thank Daniel Hicks and Alex Nunez for immunohistological support, John Fazakerley for providing his expertise on SFV, and Esther Schnettler for helping with virus production.

We have no conflicts of interest to declare with regards to this article.

REFERENCES

1. **Ransohoff RM, Engelhardt B.** 2012. The anatomical and cellular basis of immune surveillance in the central nervous system. Nat. Rev. Immunol. **12:**623–635. http://dx.doi.org/10.1038/nri3265.
2. **Kivisakk P, Mahad DJ, Callahan MK, Trebst C, Tucky B, Wei T, Wu LJ, Baekkevold ES, Lassmann H, Staugaitis SM, Campbell JJ, Ransohoff RM.** 2003. Human cerebrospinal fluid central memory CD4(+) T cells: evidence for trafficking through choroid plexus and meninges via P-selectin. Proc. Natl. Acad. Sci. U. S. A. **100:**8389–8394. http://dx.doi.org/10.1073/pnas.1433000100.
3. **Fazakerley JK.** 2002. Pathogenesis of Semliki Forest virus encephalitis. J. Neurovirol. **8:**66–74. http://dx.doi.org/10.1080/135502802901068000.
4. **Griffin DE.** 2003. Immune responses to RNA-virus infections of the CNS. Nat. Rev. Immunol. **3:**493–502. http://dx.doi.org/10.1038/nri1105.
5. **Lane TE, Liu MT, Chen BP, Asensio VC, Samawi RM, Paoletti AD, Campbell IL, Kunkel SL, Fox HS, Buchmeier MJ.** 2000. A central role for CD4(+) T cells and RANTES in virus-induced central nervous system inflammation and demyelination. J. Virol. **74:**1415–1424. http://dx.doi.org/10.1128/JVI.74.3.1415-1424.2000.
6. **Suthar MS, Diamond MS, Gale M, Jr.** 2013. West Nile virus infection and immunity. Nat. Rev. Microbiol. **11:**115–128. http://dx.doi.org/10.1038/nrmicro2950.
7. **Mantovani A.** 1999. The chemokine system: redundancy for robust outputs. Immunol. Today **20:**254–257. http://dx.doi.org/10.1016/S0167-5699(99)01469-3.
8. **Rot A, von Andrian UH.** 2004. Chemokines in innate and adaptive host defense: basic chemokinese grammar for immune cells. Annu. Rev. Immunol. **22:**891–928. http://dx.doi.org/10.1146/annurev.immunol.22.012703.104543.
9. **Zlotnik A, Yoshie O.** 2000. Chemokines: a new classification system and their role in immunity. Immunity **12:**121–127. http://dx.doi.org/10.1016/S1074-7613(00)80165-X.
10. **Graham GJ, Locati M.** 2013. Regulation of the immune and inflammatory responses by the 'atypical' chemokine receptor D6. J. Pathol. **229:**168–175. http://dx.doi.org/10.1002/path.4123.

11. **Bachelerie F, Ben-Baruch A, Burkhardt AM, Combadiere C, Farber JM, Graham GJ, Horuk R, Sparre-Ulrich AH, Locati M, Luster AD, Mantovani A, Matsushima K, Murphy PM, Nibbs R, Nomiyama H, Power CA, Proudfoot AE, Rosenkilde MM, Rot A, Sozzani S, Thelen M, Yoshie O, Zlotnik A.** 2014. International Union of Basic and Clinical Pharmacology. LXXXIX. Update on the extended family of chemokine receptors and introducing a new nomenclature for atypical chemokine receptors. Pharmacol. Rev. **66:**1–79. http://dx.doi.org/10.1124/pr.113.007724.
12. **McKimmie CS, Graham GJ.** 2010. Astrocytes modulate the chemokine network in a pathogen-specific manner. Biochem. Biophys. Res. Commun. **394:**1006–1011. http://dx.doi.org/10.1016/j.bbrc.2010.03.111.
13. **McKimmie CS, Roy D, Forster T, Fazakerley JK.** 2006. Innate immune response gene expression profiles of N9 microglia are pathogen-type specific. J. Neuroimmunol. **175:**128–141. http://dx.doi.org/10.1016/j.jneuroim.2006.03.012.
14. **Ambrosini E, Aloisi F.** 2004. Chemokines and glial cells: a complex network in the central nervous system. Neurochem. Res. **29:**1017–1038. http://dx.doi.org/10.1023/B:NERE.0000021246.96864.89.
15. **Hesselgesser J, Horuk R.** 1999. Chemokine and chemokine receptor expression in the central nervous system. J. Neurovirol. **5:**13–26. http://dx.doi.org/10.3109/13550289909029741.
16. **Hofer MJ, Carter SL, Mueller M, Campbell IL.** 2008. Unaltered neurological disease and mortality in CXCR3-deficient mice infected intracranially with lymphocytic choriomeningitis virus-Armstrong. Viral Immunol. **21:**425–433. http://dx.doi.org/10.1089/vim.2008.0057.
17. **Zhang B, Chan YK, Lu B, Diamond MS, Klein RS.** 2008. CXCR3 mediates region-specific antiviral T cell trafficking within the central nervous system during West Nile virus encephalitis. J. Immunol. **180:**2641–2649. http://dx.doi.org/10.4049/jimmunol.180.4.2641.
18. **Glass WG, McDermott DH, Lim JK, Lekhong S, Yu SF, Frank WA, Pape J, Cheshier RC, Murphy PM.** 2006. CCR5 deficiency increases risk of symptomatic West Nile virus infection. J. Exp. Med. **203:**35–40. http://dx.doi.org/10.1084/jem.20051970.
19. **Lim JK, Glass WG, McDermott DH, Murphy PM.** 2006. CCR5: no longer a "good for nothing" gene–chemokine control of West Nile virus infection. Trends Immunol. **27:**308–312. http://dx.doi.org/10.1016/j.it.2006.05.007.
20. **Nansen A, Christensen JP, Andreasen SO, Bartholdy C, Christensen JE, Thomsen AR.** 2002. The role of CC chemokine receptor 5 in antiviral immunity. Blood **99:**1237–1245. http://dx.doi.org/10.1182/blood.V99.4.1237.
21. **Klein RS, Lin E, Zhang B, Luster AD, Tollett J, Samuel MA, Engle M, Diamond MS.** 2005. Neuronal CXCL10 directs CD8(+) T-cell recruitment and control of West Nile virus encephalitis. J. Virol. **79:**11457–11466. http://dx.doi.org/10.1128/JVI.79.17.11457-11466.2005.
22. **Samuel MA, Diamond MS.** 2005. Alpha/beta interferon protects against lethal West Nile virus infection by restricting cellular tropism and enhancing neuronal survival. J. Virol. **79:**13350–13361. http://dx.doi.org/10.1128/JVI.79.21.13350-13361.2005.
23. **Shrestha B, Wang T, Samuel MA, Whitby K, Craft J, Fikrig E, Diamond MS.** 2006. Gamma interferon plays a crucial early antiviral role in protection against West Nile virus infection. J. Virol. **80:**5338–5348. http://dx.doi.org/10.1128/JVI.00274-06.
24. **McKimmie CS, Fraser AR, Hansell C, Gutierrez L, Philipsen S, Connell L, Rot A, Kurowska-Stolarska M, Carreno P, Pruenster M, Chu CC, Lombardi G, Halsey C, McInnes IB, Liew FY, Nibbs RJ, Graham GJ.** 2008. Hemopoietic cell expression of the chemokine decoy receptor D6 is dynamic and regulated by GATA1. J. Immunol. **181:**3353–3363. http://dx.doi.org/10.4049/jimmunol.181.5.3353.
25. **McKimmie CS, Moore M, Fraser AR, Jamieson T, Xu D, Burt C, Pitman NI, Nibbs RJ, McInnes IB, Liew FY, Graham GJ.** 2009. A TLR2 ligand suppresses inflammation by modulation of chemokine receptors and redirection of leukocyte migration. Blood **113:**4224–4231. http://dx.doi.org/10.1182/blood-2008-08-174698.
26. **McKimmie CS, Fazakerley JK.** 2005. In response to pathogens, glial cells dynamically and differentially regulate Toll-like receptor gene expression. J. Neuroimmunol. **169:**116–125. http://dx.doi.org/10.1016/j.jneuroim.2005.08.006.
27. **Schmittgen TD, Livak KJ.** 2008. Analyzing real-time PCR data by the comparative C-T method. Nat. Protoc. **3:**1101–1108. http://dx.doi.org/10.1038/nprot.2008.73.
28. **Cardona AE, Huang D, Sasse ME, Ransohoff RM.** 2006. Isolation of murine microglial cells for RNA analysis or flow cytometry. Nat. Protoc. **1:**1947–1951. http://dx.doi.org/10.1038/nprot.2006.327.
29. **Lee KM, McKimmie CS, Gilchrist DS, Pallas KJ, Nibbs RJ, Garside P, McDonald V, Jenkins C, Ransohoff R, Liu L, Milling S, Cerovic V, Graham GJ.** 2011. D6 facilitates cellular migration and fluid flow to lymph nodes by suppressing lymphatic congestion. Blood **118:**6220–6229. http://dx.doi.org/10.1182/blood-2011-03-344044.
30. **Mirzadegan T, Diehl F, Ebi B, Bhakta S, Polsky I, McCarley D, Mulkins M, Weatherhead GS, Lapierre JM, Dankwardt J, Morgans D, Jr, Wilhelm R, Jarnagin K.** 2000. Identification of the binding site for a novel class of CCR2b chemokine receptor antagonists: binding to a common chemokine receptor motif within the helical bundle. J. Biol. Chem. **275:**25562–25571. http://dx.doi.org/10.1074/jbc.M000692200.
31. **Du X, Gustin DJ, Chen X, Duquette J, McGee LR, Wang Z, Ebsworth K, Henne K, Lemon B, Ma J, Miao S, Sabalan E, Sullivan TJ, Tonn G, Collins TL, Medina JC.** 2009. Imidazo-pyrazine derivatives as potent CXCR3 antagonists. Bioorg. Med. Chem. Lett. **19:**5200–5204. http://dx.doi.org/10.1016/j.bmcl.2009.07.021.
32. **Johnson M, Li A-R, Liu J, Fu Z, Zhu L, Miao S, Wang X, Xu Q, Huang A, Marcus A, Xu F, Ebsworth K, Sablan E, Danao J, Kumer J, Dairaghi D, Lawrence C, Sullivan T, Tonn G, Schall T, Collins T, Medina J.** 2007. Discovery and optimization of a series of quinazolinone-derived antagonists of CXCR3. Bioorg. Med. Chem. Lett. **17:**3339–3343. http://dx.doi.org/10.1016/j.bmcl.2007.03.106.
33. **Lee YK, Choi D-Y, Jung Y-Y, Yun YW, Lee BJ, Han SB, Hong JT.** 2013. Decreased pain responses of C-C chemokine receptor 5 knockout mice to chemical or inflammatory stimuli. Neuropharmacology **67:**57–65. http://dx.doi.org/10.1016/j.neuropharm.2012.10.030.
34. **Rosi S, Pert CB, Ruff MR, McGann-Gramling K, Wenk GL.** 2005. Chemokine receptor 5 antagonist d-Ala-peptide T-amide reduces microglia and astrocyte activation within the hippocampus in a neuroinflammatory rat model of Alzheimer's disease. Neuroscience **134:**671–676. http://dx.doi.org/10.1016/j.neuroscience.2005.04.029.
35. **Polianova MT, Ruscetti FW, Pert CB, Ruff MR.** 2005. Chemokine receptor-5 (CCR5) is a receptor for the HIV entry inhibitor peptide T (DAPTA). Antiviral Res. **67:**83–92. http://dx.doi.org/10.1016/j.antiviral.2005.03.007.
36. **Bridge TP, Heseltine PR, Parker E, Eaton E, Ingraham L, Gill M, Ruff M, Pert C, Goodwin F.** 1989. Improvement in AIDS patients on peptide T. Lancet **ii:**226–227.
37. **McCandless E, Zhang B, Diamond M, Klein R.** 2008. CXCR4 antagonism increases T cell trafficking in the central nervous system and improves survival from West Nile virus encephalitis. Proc. Natl. Acad. Sci. U. S. A. **105:**11270–11275. http://dx.doi.org/10.1073/pnas.0800898105.
38. **Geissmann F, Jung S, Littman DR.** 2003. Blood monocytes consist of two principal subsets with distinct migratory properties. Immunity **19:**71–82. http://dx.doi.org/10.1016/S1074-7613(03)00174-2.
39. **Mack M, Cihak J, Simonis C, Luckow B, Proudfoot AEI, Plachý J, Brühl H, Frink M, Anders H-J, Vielhauer V, Pfirstinger J, Stangassinger M, Schlöndorff D.** 2001. Expression and characterization of the chemokine receptors CCR2 and CCR5 in mice. J. Immunol. **166:**4697–4704. http://dx.doi.org/10.4049/jimmunol.166.7.4697.
40. **Getts D, Terry R, Getts M, Muller M, Rana S, Shrestha B, Radford J, Van Rooijen N, Campbell I, King N.** 2008. Ly6c+ "inflammatory monocytes" are microglial precursors recruited in a pathogenic manner in West Nile virus encephalitis. J. Exp. Med. **205:**2319–2337. http://dx.doi.org/10.1084/jem.20080421.
41. **Lim JK, Obara CJ, Rivollier A, Pletnev AG, Kelsall BL, Murphy PM.** 2011. Chemokine receptor Ccr2 is critical for monocyte accumulation and survival in West Nile virus encephalitis. J. Immunol. **186:**471–478. http://dx.doi.org/10.4049/jimmunol.1003003.
42. **Rosler A, Pohl M, Braune HJ, Oertel WH, Gemsa D, Sprenger H.** 1998. Time course of chemokines in the cerebrospinal fluid and serum during herpes simplex type 1 encephalitis. J. Neurol. Sci. **157:**82–89. http://dx.doi.org/10.1016/S0022-510X(98)00061-6.
43. **Tigabu B, Juelich T, Holbrook MR.** 2010. Comparative analysis of immune responses to Russian spring-summer encephalitis and Omsk hemorrhagic fever viruses in mouse models. Virology **408:**57–63. http://dx.doi.org/10.1016/j.virol.2010.08.021.
44. **Hicks DJ, Núñez A, Banyard AC, Williams A, Ortiz-Pelaez A, Fooks AR, Johnson N.** 2013. Differential chemokine responses in the murine brain following lyssavirus Infection. J. Comp. Pathol. **149:**446–462. http://dx.doi.org/10.1016/j.jcpa.2013.04.001.

45. **Chen B, Kuziel W, Lane T.** 2001. Lack of CCR2 results in increased mortality and impaired leukocyte activation and trafficking following infection of the central nervous system with a neurotropic coronavirus. J. Immunol. **167:** 4585–4592. http://dx.doi.org/10.4049/jimmunol.167.8.4585.
46. **Glass WG, Chen BP, Liu MT, Lane TE.** 2002. Mouse hepatitis virus infection of the central nervous system: chemokine-mediated regulation of host defense and disease. Viral Immunol. **15:**261–272. http://dx.doi.org/10.1089/08828240260066215.
47. **Terry R, Getts D, Deffrasnes C, van Vreden C, Campbell I, King N.** 2012. Inflammatory monocytes and the pathogenesis of viral encephalitis. J. Neuroinflamm. **9:**270. http://dx.doi.org/10.1186/1742-2094-9-270.
48. **Klein RS, Diamond MS.** 2008. Immunological headgear: antiviral immune responses protect against neuroinvasive West Nile virus. Trends Mol. Med. **14:**286–294. http://dx.doi.org/10.1016/j.molmed.2008.05.004.
49. **Saederup N, Cardona AE, Croft K, Mizutani M, Cotleur AC, Tsou C-L, Ransohoff RM, Charo IF.** 2010. Selective chemokine receptor usage by central nervous system myeloid cells in CCR2-red fluorescent protein knock-in mice. PLoS One **5:**e13693. http://dx.doi.org/10.1371/journal.pone.0013693.
50. **Christensen JE, Simonsen S, Fenger C, Sorensen MR, Moos T, Christensen JP, Finsen B, Thomsen AR.** 2009. Fulminant lymphocytic choriomeningitis virus-induced inflammation of the CNS involves a cytokine-chemokine-cytokine-chemokine cascade. J. Immunol. **182:**1079–1087. http://dx.doi.org/10.4049/jimmunol.182.2.1079.
51. **Amor S, Scallan MF, Morris MM, Dyson H, Fazakerley JK.** 1996. Role of immune responses in protection and pathogenesis during Semliki Forest virus encephalitis. J. Gen. Virol. **77:**281–291. http://dx.doi.org/10.1099/0022-1317-77-2-281.
52. **Griffin DE.** 2010. Recovery from viral encephalomyelitis: immune-mediated noncytolytic virus clearance from neurons. Immunol. Res. **47:** 123–133. http://dx.doi.org/10.1007/s12026-009-8143-4.
53. **Metcalf TU, Griffin DE.** 2011. Alphavirus-induced encephalomyelitis: antibody-secreting cells and viral clearance from the nervous system. J. Virol. **85:**11490–11501. http://dx.doi.org/10.1128/JVI.05379-11.
54. **Subaksharpe I, Dyson H, Fazakerley J.** 1993. In vivo depletion of CD8+ T-cells prevents lesions of demyelination in Semliki Forest virus infection. J. Virol. **67:**7629–7633.
55. **Glass WG, Lane TE.** 2003. Functional expression of chemokine receptor CCR5 on CD4(+) T cells during virus-induced central nervous system disease. J. Virol. **77:**191–198. http://dx.doi.org/10.1128/JVI.77.1.191-198.2003.
56. **Berger EA, Murphy PM, Farber JM.** 1999. Chemokine receptors as HIV-1 coreceptors: roles in viral entry, tropism, and disease. Annu. Rev. Immunol. **17:**657–700. http://dx.doi.org/10.1146/annurev.immunol.17.1.657.
57. **Glass WG, Lim JK, Cholera R, Pletnev AG, Gao JL, Murphy PM.** 2005. Chemokine receptor CCR5 promotes leukocyte trafficking to the brain and survival in West Nile virus infection. J. Exp. Med. **202:**1087–1098. http://dx.doi.org/10.1084/jem.20042530.
58. **Horuk R.** 2009. Chemokine receptor antagonists: overcoming developmental hurdles. Nat. Rev. Drug Discov. **8:**23–33. http://dx.doi.org/10.1038/nrd2734.
59. **Schall TJ, Proudfoot AEI.** 2011. Overcoming hurdles in developing successful drugs targeting chemokine receptors. Nat. Rev. Immunol. **11:**355–363. http://dx.doi.org/10.1038/nri2972.